Handbook of Computer Networks: Key Concepts, Data Transmission, and Digital and Optical Networks
by Hossein Bidgoli

Pulse Position Modulation

Jon Hamkins, *Jet Propulsion Laboratory, California Institute of Technology, Pasadena, California*

INTRODUCTION

Pulse position modulation (PPM) is a signaling format in which the temporal positions of pulses are modulated by a message. In this chapter, we explore the history, fundamentals, and modern design principles of PPM. As we shall see, the PPM signal format has a long history and a bright future.

History

Early references to PPM in the electrical engineering literature use the term *pulse position modulation* unevenly to refer to any one of a multitude of transmission schemes in which pulse positions are modulated by a message. In several early descriptions of PPM (Lacy 1947; McAulay 1968; Riter, Boatright, and Shay 1971), the frequency of the pulses was held fixed and information was contained in the continuous variation of a pulse from its nominal position. This has been referred to as *PPM with a fixed reference* (Ross 1949); in today's terminology, it would be referred to as *analog PPM*. When the pulse positions can take on only discrete values, as is the case in modern designs, the early literature referred to the modulation as *quantized PPM* (QPPM) (Pettit 1965).

In another early scheme, the frequency of pulses was held fixed, with the center of each pulse not varying at all from the nominal frequency. The information was contained in the variation in the position of the rising (and symmetrically falling) edge of the pulse. To maintain a constant energy per pulse, the amplitude was varied inversely to the pulse width. In today's terminology, this is more properly termed *return-to-zero pulse width modulation* and *pulse amplitude modulation*.

These and other types of pulsed transmissions have been in use since at least World War II ("Pulse position" 1945) and expressed in early *private branch exchange* (PBX) implementations by AT&T (Meiseand and DeStefano 1966). Indeed, the concept of pulsed transmission is much older than that: Native Americans used it in their smoke signals, with one puff meaning "Attention," two in rapid succession meaning "All is well," and three in rapid succession meaning "Danger" or "Help" (Tomkins 2002). Several decades ago, the optical communications literature came on what is now the standard definition of PPM (Gagliardi and Karp 1976), which is a specific form of QPPM. In this chapter, to avoid confusion, we shall define and analyze PPM in only this standard way.

Applications

PPM has a rich history of applications in optical, radio frequency, and acoustical communications.

Optical Communications Links

In recent years, the dominant application of PPM has been optical communications. PPM has long been suggested for use in optical systems because its potential for a high peak-to-average power ratio naturally fits the physical properties of lasers, which may emit a pulse of light with a high peak power but which output a much lower average power. Such a property has been shown to be an efficient means of transmitting at high data rates, even when background light interferes.

Using PPM, a laser sends a pulse of light delayed in proportion to the value of the message being transmitted. The light pulses can be either transmitted through free space, including to and from outer space (Wilson and

Lesh 1993; Wilson et al. 1997; Townes et al. 2004), or coupled to an optical fiber (Palais 2004; Ohtsuki and Kahn 2000). The receiver detects the delay of the light pulse to decipher the intended message. [In the case of earlier demonstrations (Wilson and Lesh 1993; Wilson et al. 1997) pulse lasers were used, but not PPM specifically.]

In one impressive PPM application, NASA developed technology for high-speed optical transmission from a Mars orbiter, originally set to launch in 2009, to Earth (Townes et al. 2004). The system supports data rates as high as 50 Mbps over a distance of 150 million kilometers using a laser with an average output power of 5 W, which is one hundred times faster than Mars–Earth data rates achieved as of this writing. The link design uses 32-ary and 64-ary PPM (Moision and Hamkins 2003), depending on link conditions, highly accurate pointing algorithms (Lee, Ortiz, and Alexander 2005), reception with either the 5-meter Hale telescope on Palomar Mountain or an array of smaller telescopes (Candell 2005), efficient photodetectors (Biswas and Farr 2004), and a specially developed *error-correction code* (ECC) that operates within 1 decibel (dB) of the Shannon limit (Moision and Hamkins 2005, "Coded"). Laboratory demonstrations showed the proper operation of a multi-Mbps end-to-end system under expected link conditions, but a new emphasis on human flight missions within NASA has forced the cancellation of this robotic mission.

Another free space optical application that uses PPM is the infrared links for the consumer mobile electronics devices that are becoming ubiquitous. The Infrared Data Association has developed the IrDa standard (Knutson and Brown 2004) which includes, among other modes, a "fast infrared" mode that operates at 4 Mbps using 4-ary PPM. Laptop computers, cell phones, personal information managers, cameras, printers, and many other consumer devices now have IrDa-compliant transceivers. Infrared television remote controls do not typically use the IrDa standard, but they often operate with a type of PPM as well (Casier, De Man, and Matthijs 1976). For example, JVC, Mitsubishi, NEC, Philips, Sanyo, Sharp, and Toshiba manufacture televisions that use PPM as the format for infrared remote control. An NEC data sheet (NEC Corporation 1994) contains a description of a representative signaling format.

Remotely Controlled Vehicles

Remotely controlled aircraft, watercraft, vehicles, and robots routinely use PPM as a method of accurately obtaining controlling information from the operator. Signals transmitted with radio frequency pulses have time delays that are proportional to several controls (e.g., the angles of ailerons, elevators, and rudder and steering and throttles) that the operator desires to set.* PPM is chosen for this application because the vehicles and vessels require low-complexity receivers (especially aircraft), and the electronics needed to convert a pulse to a motor position are simple.

Medical Sensors

A sensor may be implanted in or attached externally to medical patients who require close monitoring of blood pressure, blood flow, temperature, the presence of certain chemicals, and the vital signs of a baby during birth. The sensor can transmit radio waves to a remote receiver that displays or records the data. PPM is an efficient transmission for this application, particularly for analog data such as these, thereby providing the longest possible battery life before inconvenient sensor replacement (Bornhoft et al. 2001).

Oil and Coal Drilling

Drilling is necessary in both the oil and coal industries for both exploration and methane drainage. Automatic monitoring of the borehole trajectory, bit thrust, and torque during drilling assists greatly in drilling the longest, straightest, and most accurately aimed holes. To do this, so-called measure-while-drilling or logging-while-drilling techniques are used, by which pressure pulses in the drilling fluid are modulated with PPM at the end of the drill bit down the hole and detected at the surface (Marsh et al. 2002).

Underwater Acoustic Communications Links

PPM can also be used for acoustic underwater signaling. A short acoustical tone is transmitted with a delay that is a linear function of the value being sent (Riter, Boatright, and Shay 1971). In addition to ocean communication on Earth, this technique has been considered for the exploration of Europa, a moon of Jupiter with a thin layer of ice and liquid water beneath. In this mission scenario, a probe would penetrate the surface and communicate with acoustic PPM back to a surface spacecraft.

FUNDAMENTALS OF PPM

Definition of PPM

PPM is a modulation format that maps message bits to pulse positions. In the modern use of the term, a PPM *symbol* comprises M slots, exactly one of which contains a pulse. Input message bits determine which of the M positions is used. For the simplest mapping, M is typically taken to be a power of 2, in which case $\log_2 M$ message bits specify one of the M possible positions of the pulse, as shown in Figure 1. If the slots are numbered $0, 1, \ldots, M-1$, then in the mapping shown in Figure 1, the decimal representation of the bits is the number of the slot containing the pulse. As a shorthand, M-ary PPM is often referred to as M-PPM (not to be confused with *multipulse* PPM, or MPPM, discussed later in this chapter).

Mathematically, M-ary PPM may be described as the encoding of a k-bit source $\mathbf{U} = (U_1, \ldots, U_k) \in \{0,1\}^k$ to yield a signal $\mathbf{X} = (0, \ldots, 0, 1, 0, \ldots, 0) \in \{0,1\}^M$, $M = 2^k$, which contains a single one in the position indicated by the decimal representation of $\mathbf{U}$.

*In 1898, Nikola Tesla was issued the first patent (U.S. patent 613, 809) for remote-controlled vessels. The patent, however, primarily concerns the mechanical positions of brushes and contact plates and does not propose PPM. The controlling actions are made by directly rendering a given circuit either active or inactive, according to the signal transmitted from a remote operator.

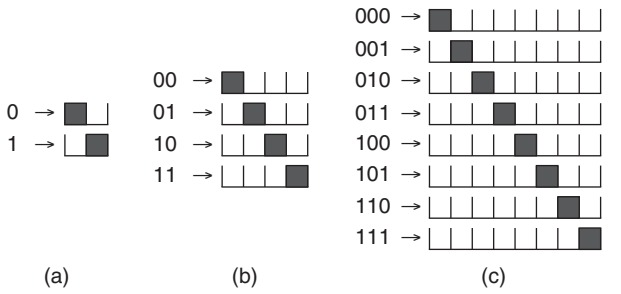

Figure 1: *M*-ary PPM maps $\log_2 M$ bits to a pulse in one of *M* positions—(a) binary PPM, (b) 4-ary PPM, (c) 8-ary PPM

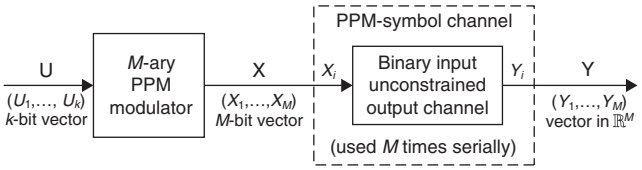

Figure 2: Block diagram of PPM modulator and memoryless channel

PPM Channel Model

To facilitate the analysis in this chapter, we now formalize a description of the channel model. The transmission channel for each slot, the *slot channel*, is a binary-input unconstrained-output channel, with input $X \in \{0,1\}$ and output $Y \in \mathbb{R}$. When no pulse is transmitted in a slot, $X = 0$; and when a pulse is transmitted in a slot, $X = 1$. We define $f_{Y|X}(y|x)$ as the *conditional probability density* (or mass) of receiving $Y = y$ in a slot, given $X = x$.

The PPM symbol $\mathbf{X} = (X_1, \ldots, X_M)$ is transmitted via M uses of the slot channel and results in the received vector $\mathbf{Y} = (Y_1, \ldots, Y_M) \in \mathbb{R}^M$. This is illustrated in Figure 2. We let $S = \{\mathbf{x}_1, \ldots, \mathbf{x}_M\}$ be the set of M-PPM symbols. Each $\mathbf{x}_k = (x_{k,1}, \ldots, x_{k,M})$ is a binary M-vector with one 1 in position k, and $M - 1$ zeros in all other positions. We define $f_{\mathbf{Y}|\mathbf{X}}(\mathbf{y}|\mathbf{x})$ as the conditional probability density of receiving $\mathbf{Y} = \mathbf{y}$ in the M slots, given $\mathbf{X} = \mathbf{x}$.

If the slot channel is memoryless, then every slot of the transmission is conditionally independent of every other slot, given the transmitted sequence. In other words, if PPM symbols $\underline{\mathbf{x}} = (\mathbf{x}^{(1)}, \ldots, \mathbf{x}^{(N)})$ are transmitted, where each symbol $\mathbf{x}^{(i)} \in S$ is a binary M-vector as described above, then the conditional probability or probability density of receiving the real M-vector $\underline{\mathbf{y}} = (\mathbf{y}^{(1)}, \ldots, \mathbf{y}^{(N)})$ factors over the symbols and slots as

$$f_{\underline{\mathbf{Y}}|\underline{\mathbf{X}}}(\underline{\mathbf{y}}|\underline{\mathbf{x}}) = \prod_{i=1}^{N}\prod_{j=1}^{M} f_{Y_j^{(i)}|X_j^{(i)}}(y_j^{(i)}|x_j^{(i)}) \tag{1}$$

For this type of channel, there is no intersymbol interference and no interslot interference. If the slot channel is also stationary, then each factor in Equation 1 simplifies to $f_{Y|X}(y_j^{(i)}|x_j^{(i)})$.

The likelihood ratio of receiving value y in a slot is denoted by $L(y) \triangleq \dfrac{f_{Y|X}(y|1)}{f_{Y|X}(y|0)}$, which for algebraic convenience we assume to be finite for all y. We also assume that $L(y)$ is monotonic in y, as is the case for many channels of practical interest (e.g., Poisson, Gaussian, and Webb-McIntyre-Conradi) (Vilnrotter, Simon, and Srinivasan 1999). The log-likelihood ratio is denoted $\Lambda(y) = \log L(y)$. $F_{Y|X}(y|1)$ ($F_{Y|X}(y|0)$) denotes the cumulative distribution—that is, the probability that a received signal (nonsignal) slot has value less than or equal to y.

Several common probability densities arise in PPM applications. Perhaps the most common is the Poisson distribution, which arises for optical communications:

$$f_{Y|X}(k|0) = \frac{K_b^k e^{-K_b}}{k!}, k \in \{0\} \cup \mathbb{N} \tag{2}$$

$$f_{Y|X}(k|1) = \frac{(K_s + K_b)^k e^{-(K_s+K_b)}}{k!}, k \in \{0\} \cup \mathbb{N} \tag{3}$$

where K_b is the average number of background photons detected when $X = 0$ and $K_s + K_b$ is the average number of signal and background photons detected when $X = 1$. Several other models for optical communications may arise, depending on whether the system is limited by shot noise or thermal noise; whether the photodetector is a PIN diode, a *photomultiplier tube* (PMT), or an *avalanche photodiode detector* (APD); and which of various approximations are used. The equations governing these models are discussed in depth in Dolinar et al. (2006) and Gagliardi and Karp (1995) and summarized here in Table 1. In each case, m_0 and σ^2_0 denote the mean and variance conditioned on $X = 0$, and m_1 and σ^2_1 denote the corresponding quantities conditioned on $X = 1$. We define the slot *signal-to-noise ratio* (SNR) as $\beta = (m_1 - m_0)^2/\sigma^2_0$, the "excess SNR" as $\gamma = (m_1 - m_0)^2/(\sigma^2_1 - \sigma^2_0)$, and the "bit SNR" as $\beta_b = \beta/(2R_c \log_2 M)$, where R_c is the ECC code rate ($R_c = 1$ if uncoded).

Bit-to-PPM Symbol Mappings

Figure 1 shows one mapping of user bits to pulse positions. We refer to this as a *bit-to-symbol* mapping. Each $\log_2 M$ bit corresponds to one PPM symbol. There are many choices—indeed, $M!$ choices—for the bit-to-symbol mapping. One question naturally arises: What is the best choice of the bit-to-symbol mapping?

If we suppose, as is consistent with typical applications, that the slot channel is either slowly varying or stationary, then we arrive at a convenient result: The performance of the system is equivalent under every bit-to-symbol mapping. To see this, we note that one bit-to-symbol mapping can be obtained from any other bit-to-symbol mapping by a suitable reordering of the coordinates of the transmitted slots. For example, if bits 11 are mapped to PPM symbol (0,0,0,1) in one bit-to-symbol mapping and to (0,1,0,0) in another, then we may transform the first mapping to the second, in part, by moving the fourth slot to the second position. Because the channel is stationary and the slots are conditionally independent, the reordering does not affect the statistics of the channel, and the performance will be the same.

In this situation, the choice of bit-to-symbol mapping is made for the convenience of the implementation.

Table 1: Probability mass functions probability density functions of several optical channel models*

Channel model	pmf or pdf
Poisson	$f_{Y\|X}(k\|x) = \frac{m_x^k e^{-m_x}}{k!}$, where $m_0 = K_b, m_1 = K_s + K_b, k \in \{0\} \cup \mathbb{N}$,
AWGN	$f_{Y\|X}(y\|x) = \frac{1}{\sigma_x}\phi\left(\frac{y-m_x}{\sigma_x}\right), y \in \mathbb{R}$, where $\phi(x) = \frac{1}{\sqrt{2\pi}} e^{-x^2/2}$
McIntyre−Conradi**	$f_{Y\|X}(k\|x) = \sum_{n=1}^{k} \frac{n\Gamma\left(\frac{k}{1-k_{eff}}+1\right)\left[\frac{1+k_{eff}(G-1)}{G}\right]^{n+k_{eff}k/(1-k_{eff})}\left[\frac{(1-k_{eff})(G-1)}{G}\right]^{k-n} K_x^n e^{-K_x}}{k(k-n)!\Gamma\left(\frac{k_{eff}k}{1-k_{eff}}+n+1\right)n!}$
WMC**	$f_{Y\|X}(y\|x) = \frac{1}{\sqrt{2\pi\sigma_x^2}}\left(1+\frac{y-m_x}{\sigma_x\delta_x}\right)^{-3/2} \exp\left[-\frac{(y-m_x)^2}{2\sigma_x^2\left(1+\frac{y-m_x}{\sigma_x\delta_x}\right)}\right], y \in \mathbb{R}$
WMC +Gaussian	$f_{Y\|X}(y\|x) = \int_{m_x-\delta_x\sigma_x}^{\infty} \frac{1}{\sqrt{2\pi\sigma_n^2}} \exp\left[-\frac{(y-t)^2}{2\sigma_n^2}\right] \cdot \frac{1}{\sqrt{2\pi\sigma_x^2}}\left(1+\frac{t-m_x}{\sigma_x\delta_x}\right)^{-3/2} \exp\left[-\frac{(y-m_x)^2}{2\sigma_x^2\left(1+\frac{t-m_x}{\sigma_x\delta_x}\right)}\right] dt$

*In each case, for $x \in \{0,1\}$, m_x and σ_x^2 are the mean and variance when $X = x$, respectively
**Webb, McIntyre, and Conradi 1974

Table 2: Common Bit-to-Symbol Mappings for 8-ary PPM

Natural	Gray	Anti-Gray	PPM pulse position
000	000	000	0
001	001	111	1
010	011	001	2
011	010	110	3
100	110	011	4
101	111	100	5
110	101	010	6
111	100	101	7

The typical mapping is the *natural* mapping, in which the decimal representation of the bits is equal to the slot position of the pulse in the PPM symbol. The natural mapping is shown in Figure 1 and in Table 2.

Many applications, especially high-speed applications, risk interslot interference. This occurs, for example, when a laser pulse width is wider than a slot epoch, or when the detector bandwidth is not sufficiently high to prevent the detected pulse from spreading across slot boundaries. This introduces memory into the channel, and equation 1 no longer holds. In addition, the choice of the symbol mapping affects performance.

For uncoded PPM on a channel with interslot interference, a PPM symbol with a pulse in the ith position is generally more likely to be incorrectly detected as having a pulse in the $(i-1)$th or $(i+1)$th position than in any other position. Thus, a *Gray code* mapping (Gray 1953) helps reduce the bit error rate. A Gray code has the property that adjacent PPM symbols correspond to input bits that differ in at most one position, as seen in Table 2. For example 00,01,11,10 is a Gray code. PPM symbol errors that are off by only one slot result in only one bit error when a Gray code is used, instead of an average of $M(\log_2 M)/(2(M-1))$ bit errors that would result from a symbol error in a system employing a random bit-to-symbol mapping.

There are many distinct Gray code labelings (Agrell et al. 2004), but, to good approximation, all Gray codes have the same performance. One common and easily constructed Gray code is the *binary-reflected Gray code*. This code of size n bits is built from the code of size $n-1$ bits by appending a copy of the code in reverse order and prepending a 0 to the original code and a 1 to the new copy. For example, the Gray code 00,01,11,10 is copied in reverse order (10,11,01,00) and prepended with a 1, becoming the Gray code 000,001,011,010,110,111,101,100, as shown in Table 2.

Coded PPM refers to a system in which the input to the bit-to-symbol mapper has been previously encoded by an ECC. When coded PPM is used on a channel with interslot interference, often the opposite bit-to-symbol effect is needed, namely, the property that adjacent PPM symbols correspond to input bits that differ in as *many* positions as possible. Loosely speaking, the reason for this is that the ECC and PPM detectors work best when they complement each other, with the PPM detector determining roughly where the pulse is within a few slot positions and the structure of the ECC determining the specific slot position. If adjacent ECC code words correspond to slots that are in near proximity, neither the ECC nor the PPM detector can determine the correct slot exactly.

Therefore, a good bit-to-symbol mapping for coded PPM is often an *anti-Gray mapping*, in which adjacent M-ary PPM symbols correspond to input bits that differ in either $\log_2 M$ or $\log_2(M-1)$ bit positions. An anti-Gray code may be constructed from the binary-reflected

Gray code using the following method. Beginning with the first half of the Gray code (the words beginning with a 0), insert after each word its 1's complement negation (bitwise exclusive OR with the all 1's). In the original Gray code, words are all distinct, and all have a zero in the first position; therefore, the words in the anti-Gray code are also distinct. This mapping is shown in Table 2.

System Design Considerations

The bandwidth, power, efficiency, and throughput of a PPM system are interrelated parameters. Proper design of a near-optimal PPM system requires a careful examination of these parameters (Moision and Hamkins 2003; Hamkins and Moision, 2005) and a well-defined system optimization metric.

A *bandwidth constraint* is a limitation on the minimum slot width, T, in order to eliminate, or allow only a given level of, *intersymbol interference* (ISI). A *peak power constraint* is a limitation on the power within slots containing a signal. For example, for the optical Poisson channel, the peak power is $K_s hc/(\lambda T)$ W, because there are an average of K_s photons in the signal slot of duration T seconds and each photon has energy hc/λ J, where λ m is the wavelength of the photon, $h = 6.626 = 10^{-34}$J · s is Planck's constant, and $c = 3 \times 10^8$ m/s is the speed of light. An average power constraint is a limitation on the average power over all slots, or, in this same example, $K_s hc/(\lambda MT)$. The photon efficiency of the system is the number of bits per photon that the system achieves, or $R_c \log_2 M/K_s$ bits/photon, where R_c is the code rate of the ECC ($R_c = 1$, if uncoded). The throughput of the system is $R_c \log_2 M/(MT)$ bits/s.

An example helps illustrate a potential pitfall of the PPM system design. Suppose photon efficiency were paramount in an optical PPM system. Then the design naturally leads one to using a very large PPM order M, because photon efficiency $R_c \log_2 M/K_s$ is increasing in M. Intuitively, this makes sense, because a pulse is rarely sent (only 1 out of M slots), but it represents many ($\log_2 M$) bits. However, if there is a limited bandwidth, then increasing M necessarily reduces the data rate. Furthermore, if the peak power is limited, then increasing M reduces the average power as well (because $\log_2 M/M$ is decreasing), which can increase the error rate of the system.

The example above shows one reason why a penchant for maximizing photon efficiency, or any other single system parameter, can be a mistake. A better question to ask is, Within the power and bandwidth constraints of a system, what is the highest throughput that can be reliably achieved with a coded PPM system of acceptable implementation complexity? The answer to this can be found by following a series of steps:

1. Determine the average power, peak power, bandwidth, and implementation complexity limitations of the system.
2. Set the slot width equal to the minimum allowed by the bandwidth and complexity constraints.
3. Compute the capacity of the PPM channel under these constraints, for various PPM orders M, and identify the PPM order M^* having the highest capacity, and the corresponding data rate in bits per second or bits per slot.
4. Design an ECC, and associated encoder and decoder, with performance near the capacity of M*-ary PPM.

In some applications, such as deep space communications where the received signal is especially weak, the use of ECC is essential, and the procedure above is necessary to arrive at a successful design. On the other hand, for other applications, such as remote-controlled aircraft, signaling on fiber-optic cabling, and the mining and medical applications, signal power may not be an issue, and instead simplicity considerations may dominate the link design.

DETECTION OF PPM SIGNALS

Maximum Likelihood Detection of Uncoded PPM

After observing $\mathbf{Y} = (Y_1, \ldots, Y_M)$, the receiver must decide which PPM symbol $\mathbf{X} \in S$ was sent. The decision rule that minimizes the probability of error is the *maximum a posteriori* (MAP) rule, given by $\text{argmax}_{\mathbf{x}} f_{\mathbf{X}|\mathbf{Y}}(\mathbf{x}|\mathbf{y})$. When the symbols are sent with equal likelihood, an application of Bayes's rule implies that the MAP decision is equivalent to the *maximum likelihood* (ML) decision, given by

$$\hat{\mathbf{X}} = \underset{\mathbf{x}}{\text{argmax}}\, f_{\mathbf{Y}|\mathbf{X}}(\mathbf{y}|\mathbf{x}) \tag{4}$$

On a memoryless stationary channel, the conditional probability (or probability density) of receiving $\mathbf{Y} = \mathbf{y}$, given $\mathbf{X} = \mathbf{x}_k$, is

$$\begin{aligned} f_{\mathbf{Y}|\mathbf{X}}(\mathbf{y}|\mathbf{x}_k) &= f_{\boldsymbol{Y}|\boldsymbol{X}}(y_k|1)\left(\prod_{i\neq k} f_{\boldsymbol{Y}|\boldsymbol{X}}(y_i|0)\right) \\ &= \frac{f_{Y|X}(y_k|1)}{f_{Y|X}(y_k|0)}\left(\prod_{i=1}^{M} f_{Y|X}(y_i|0)\right) \end{aligned}$$

The ML symbol decision rule is $\hat{\boldsymbol{X}} = \boldsymbol{X}_{\hat{k}}$, where

$$\hat{k} = \underset{k}{\text{argmax}}\, f_{\mathbf{Y}|\mathbf{X}}(\mathbf{y}|\mathbf{x}_k) = \underset{k}{\text{argmax}}\, L(y_k) = \underset{k}{\text{argmax}}\, y_k \tag{5}$$

and where we made use of the monotonicity of the likelihood ratio. Equation 5 is maximized by the index k corresponding to the largest slot value—that is, the ML detection rule is to choose the symbol corresponding to the largest observed slot value. The rule has also been generalized to hold for multipulse PPM on a Poisson channel (Georghiades 1994) and arbitrary discrete memoryless channels (Hamkins and Moision 2005), as well as for even more general modulations (Hamkins et al. 2004).

Maximum Likelihood Detection of Coded PPM

A block of N PPM symbols (each a binary vector of length M) is an element of the Cartesian product $S^N = S \times \cdots \times S$. A block code is a subset $\mathcal{C} \subset S^N$. When codeword from

C are transmitted on the channel, the ML codeword decision is the codeword $\underline{\mathbf{x}} \in C$. that maximizes Equation 1. Following the same method as in the uncoded case above, the ML decision is $\hat{\underline{\mathbf{X}}} = (\mathbf{x}_{\hat{k}_1}, \ldots, \mathbf{x}_{\hat{k}_N})$ where $\hat{\underline{k}}$ is given by

$$\hat{\underline{k}} = \underset{\underline{k}:\left(\mathbf{x}_{k_1}, \ldots, \mathbf{x}_{k_N}\right) \in C}{\operatorname{argmax}} \prod_{i=1}^{N} f_{\mathbf{Y}|\mathbf{X}}\left(\boldsymbol{y}^{(i)} | \mathbf{x}_{k_i}\right) \tag{6}$$

$$= \underset{\underline{k}:\left(\mathbf{x}_{k_1}, \ldots, \mathbf{x}_{k_N}\right) \in C}{\operatorname{argmax}} \prod_{i=1}^{N} L\left(y_{k_i}^{(i)}\right) \tag{7}$$

$$= \underset{\underline{k}:\left(\mathbf{x}_{k_1}, \ldots, \mathbf{x}_{k_N}\right) \in C}{\operatorname{argmax}} \log \prod_{i=1}^{N} L\left(y_{k_i}^{(i)}\right) \tag{8}$$

$$= \underset{\underline{k}:\left(\mathbf{x}_{k_1}, \ldots, \mathbf{x}_{k_N}\right) \in C}{\operatorname{argmax}} \sum_{i=1}^{N} \Lambda\left(y_{k_i}^{(i)}\right) \tag{9}$$

In other words, the ML rule chooses the PPM code word that maximizes the sum of the log-likelihood ratios of its pulsed slots. As can be seen from Equation 9, the ML decision requires storing all of the slot values from all of the symbols in the block. This is called a *soft decision decoder.* Maximum likelihood decoding of modern codes is usually too complex to be practical, and instead the codes are decoded using suboptimal methods. On the other hand, Equation 9 demonstrates that the set of slot likelihood ratios is a sufficient statistic for ML decoding. Turbo codes, turbo-like codes, and low-density parity check codes are each decoded using slot likelihood ratios (Benedetto et al. 1996) and an iterative algorithm that attempts to approximate the ML decoder, typically with good results.

A lower complexity decoder results when symbol decisions are made first and then fed into the decoder. In this *hard decision decoder,* an initial vector of k's are made according to Equation 5—that is, using symbol-by-symbol decisions—and these are fed to the decoder, which attempts to correct the errors. This is the method used in a conventional decoder for a Reed-Solomon code, for example. An additional penalty, generally of approximately 2 dB, results from using a hard decision decoder compared to a soft decision decoder.

PERFORMANCE OF PPM

We now derive general formulas for the PPM *symbol error rate* (SER) and *bit error rate* (BER), as a function of the channel statistics $f_{Y|X}(y|x)$. The derivation assumes that the channel is memoryless and stationary, and that slot and symbol timing are perfectly known.

Symbol Error Rate and Bit Error Rate of Uncoded PPM

On a continuous-output memoryless channel, the PPM symbol error probability, P_s, is the well-known performance (Gallager 1968) of an ML detector for M-ary orthogonal signaling:

$$\begin{aligned} P_s &= 1 - \Pr(Y_1 = \max\{Y_1, \ldots, Y_M\} | X_1 = 1) \\ &= 1 - \int_{-\infty}^{\infty} f_{Y|X}(y|1) \left[\int_{-\infty}^{y} f_{Y|X}(y'|0)\, dy' \right]^{M-1} dy \end{aligned} \tag{10}$$

Equation 10 may be evaluated numerically by first producing a table lookup for the bracketed term and then computing the outer integral numerically in the usual way (Press et al. 1992).

When the channel outputs take on discrete values, there is a possibility of a tie for the maximum count. Suppose a value of k is detected in the slot containing the pulse, l nonsignal slots also have count k, and the remaining nonsignal slots have count strictly less than k. Then the correct decision is made with probability $1/(l + 1)$. Otherwise, an error is made. By summing over all possible values of k and l, it follows that

$$\begin{aligned} P_s = 1 - \sum_{k=0}^{\infty} \sum_{l=0}^{M-1} & \Pr\left[\begin{array}{l}\text{correct decision when } l \\ \text{nonsignal slots tie the signal slot for the maximum} \\ \text{count}\end{array}\right] \\ & \times \Pr\left[\begin{array}{l}\text{exactly } l \text{ of } M-1 \\ \text{nonsignal slots have} \\ \text{value } k, \text{ all others} \\ \text{smaller}\end{array}\right] \times \Pr\left[\begin{array}{l}\text{signal slot} \\ \text{has value } k\end{array}\right] \end{aligned} \tag{11}$$

$$\begin{aligned} &= 1 - \sum_{k=0}^{\infty} \sum_{l=0}^{M-1} \frac{1}{l+1} \binom{M-1}{l} f_{Y|X}(k|0)^l F_{Y|X} \\ &\quad \times (k-1|0)^{M-l-1} f_{Y|X}(k|1) \end{aligned} \tag{12}$$

An extension of Equation 12 to n-pulse PPM, $n \geq 2$, is straightforward and involves a triple summation in place of the double summation (Hamkins and Moision 2005). After some algebraic manipulation, Equation 12 can be rewritten in a single summation as (Hamkins 2004)

$$P_s = 1 - \frac{1}{M} \sum_{k=0}^{\infty} L(k) \left(F_{Y|X}(k|0)^M - F_{Y|X}(k-1|0)^M\right) \tag{13}$$

where $L(k)$ is the likelihood ratio. On a noiseless channel, $f_{Y|X}(0 \mid 0) = 1$, and the erasure probability is $f_{Y|X}(0|1)$; thus, Equation 13 can be simplified to

$$P_s = \frac{(M-1) f_{Y|X}(0|1)}{M} \tag{14}$$

This is consistent with the fact that the symbol decision (guess) is wrong $M - 1$ out of M times when no signal is received.

Once the PPM symbol is detected, it is mapped to a string of $\log_2(M)$ bits via the inverse of the encoding mapping (see Table 2). There are $M/2$ symbol errors that will produce an error in a given bit in the string, and there are $M - 1$ unique symbol errors. Thus, assuming all symbol errors are equally likely, the resulting BER is

$$P_b = \frac{M}{2(M-1)} P_s \tag{15}$$

where P_s is given by Equation 10 or Equation 13.

We now proceed to evaluate the error-rate expressions above for a couple of specific channel models: the

Poisson channel and the *additive white Gaussian noise* (AWGN) channel. The reader is reminded that the error rates derived here assume perfect slot and symbol timing and a memoryless, stationary channel. If timing jitter or intersymbol interference were present, for example, then performance would degrade.

Poisson Channel

For $K_b > 0$, the SER in Equation 13 becomes

$$P_s = 1 - \sum_{k=0}^{\infty} \left(1 + \frac{K_s}{K_b}\right)^k \frac{e^{-K_s}}{M} \left(F_{Y|X}(k|0)^M - F_{Y|X}(k-1|0)^M\right) \tag{16}$$

where $F_{Y|X}(k|0) = \sum_{m=0}^{k} \frac{K_b^k e^{-K_b}}{k!}$. When $K_b = 0$, from Equation 14 we have

$$P_s = \frac{(M-1)e^{-K_s}}{M} \tag{17}$$

and from Equation 15 we see that $P_b = \frac{1}{2}e^{-K_s}$, which is independent of M and equal to that of on-off keying. This is shown in Figure 3a. As K_b increases, the dependence on M grows and the performance for each M degrades, as seen in Figure 3b and 3c. It is not appropriate to interpret performance versus K_s as a measure of power efficiency, however. K_s is proportional to the *peak* power. The average transmitter power is proportional to K_s/M photons per slot. Whereas low values of M in Figure 3a, 3b, and 3c produce a lower BER compared to high values of M, the situation is reversed in Figure 3d, 3e, and 3f, which plot versus K_s/M. The performance is also shown relative to the photon efficiency, $\log_2 M/K_s$ bits/photon, in Figure 3g, 3h, and 3i, where it is also seen that high values of M are more photon efficient. Note that there is an average

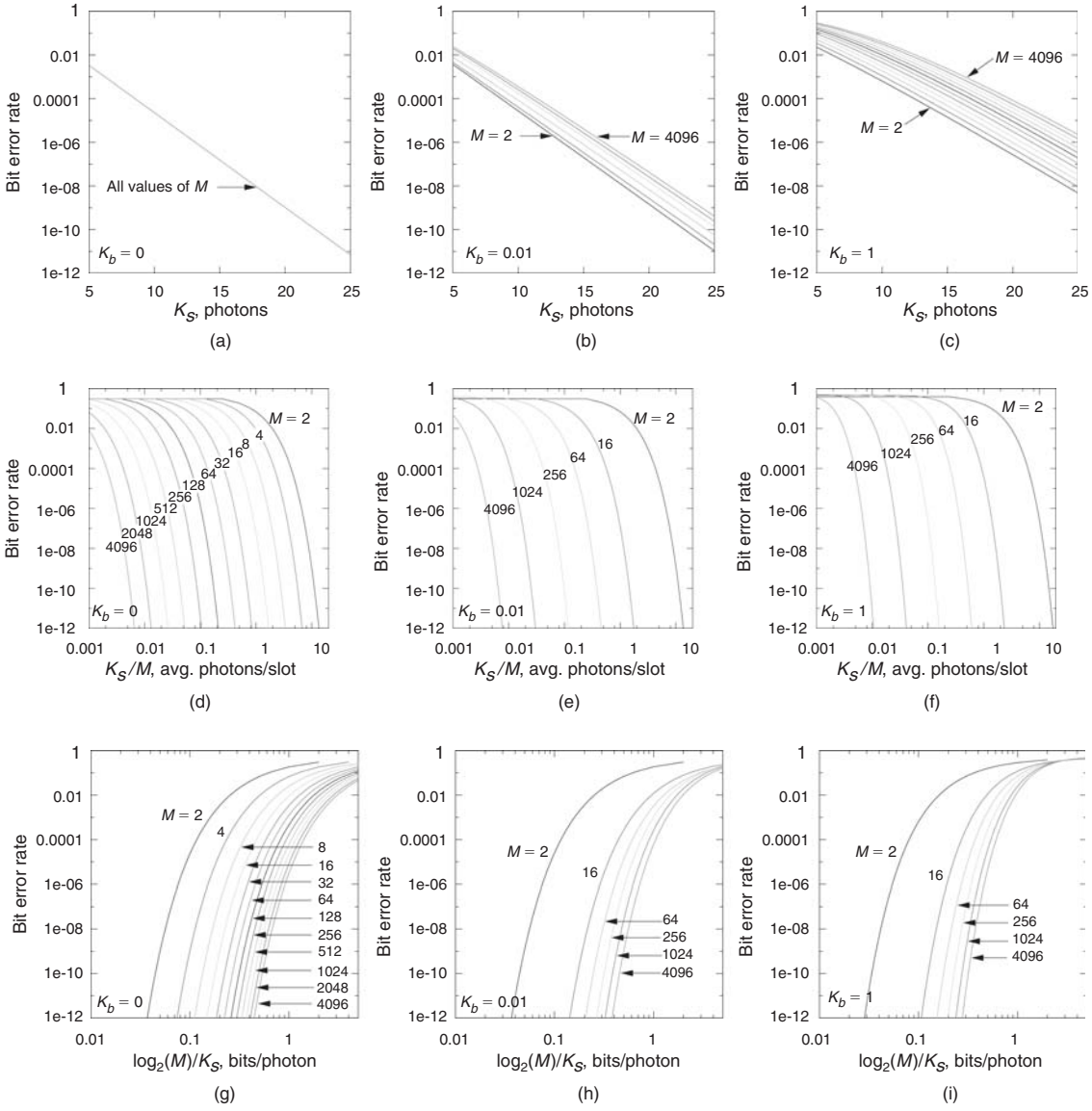

Figure 3: BER of uncoded *M*-PPM signaling on a Poisson channel versus quantities proportional to peak power (a, b, and c), average power (d, e, and f), and photon efficiency (g, h, and i) for $M = 2$ to 4096 and $K_b = 0,0.01,1$

power difference of approximately 30 dB between $M = 2$ and $M = 4096$ (Figure 3d, 3e, and 3f) and a photon-efficiency difference of approximately 10 dB (Figure 3g, 3h, and 3i). The performance is also shown in terms of the slot SNR $\beta = K_s^2/K_b$ in Figure 4a through 4d, where we see little dependence on M; when plotted in terms of the bit SNR $\beta_b = K_s^2/(2K_b \log_2 M)$, the 30 dB gap manifests itself again.

AWGN Channel

The probability of symbol error is given by Equation 10, which becomes

$$P_s = 1 - \int_{-\infty}^{\infty} \frac{1}{\sigma_1} \phi\left(\frac{x - m_1}{\sigma_1}\right) \Phi\left(\frac{x - m_0}{\sigma_0}\right)^{M-1} dx \quad (18)$$

$$= 1 - \int_{-\infty}^{\infty} \sqrt{\frac{\gamma}{\beta + \gamma}} \phi\left(\sqrt{\frac{\gamma}{\beta + \gamma}}\left((\upsilon - \sqrt{\beta}\right)\right) \Phi(\upsilon)^{M-1} d\upsilon \quad (19)$$

where $\phi(x) = \frac{1}{\sqrt{2\pi}} e^{-x^2/2}$ is the standard normalized Gaussian probability density function, $\Phi(x)$ is its cumulative distribution function, and, as defined earlier, $\beta = (m_1 - m_0)^2/\sigma_0^2$ and $\gamma = \dfrac{(m_1 - m_0)^2}{\sigma_1^2 - \sigma_0^2}$. If $\sigma_1 = \sigma_0$, then $\gamma = \infty$ and Equation 19 simplifies to

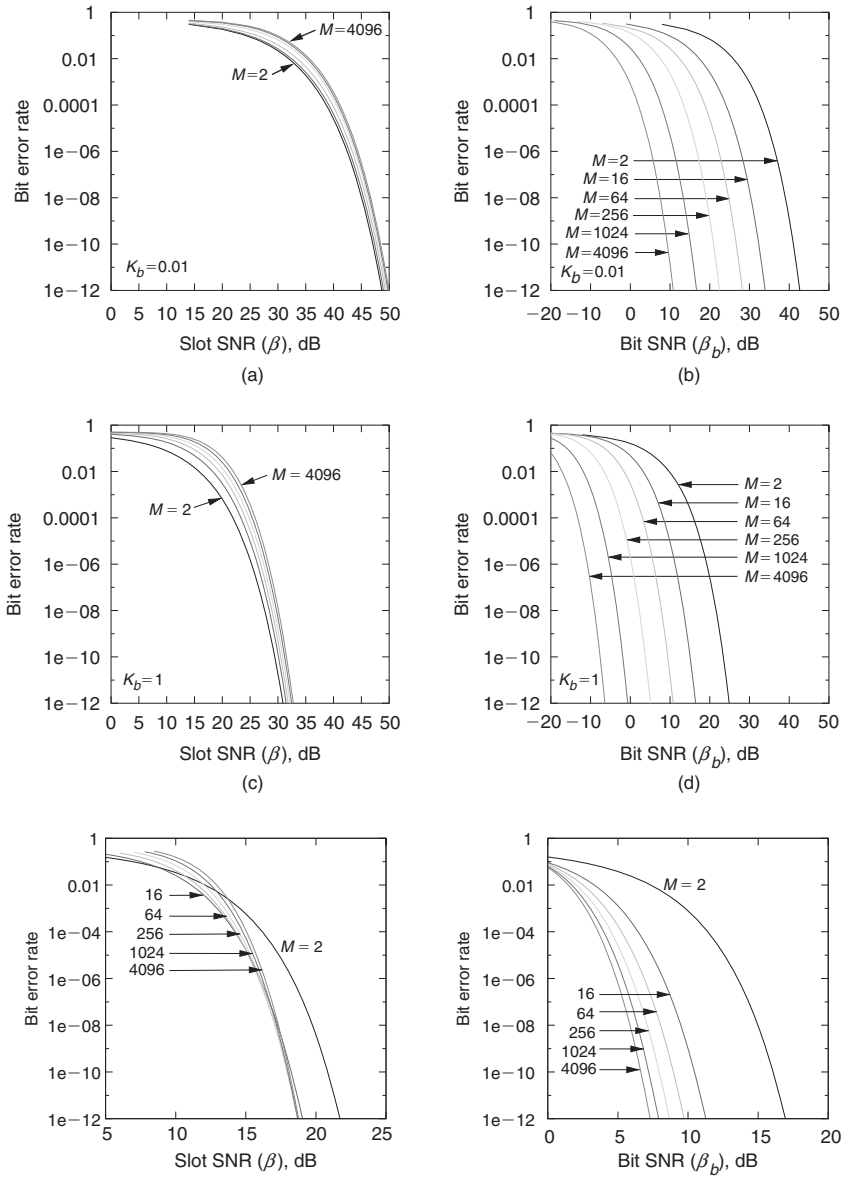

Figure 4: BER of uncoded M-PPM signaling—(a) Poisson channel versus slot SNR, (b) Poisson channel versus bit SNR, (c) Poisson channel versus slot SNR, (d) Poisson channel versus bit SNR, (e) AWGN channel versus slot SNR, and (f) AWGN channel versus bit SNR

$$P_s = 1 - \int_{-\infty}^{\infty} \phi\left(x - \sqrt{\beta}\right) \Phi(x)^{M-1} dx \qquad (20)$$

The BER P_b is then given by Equation 15 and can be expressed in terms of the bit SNR $\beta_b = \beta/(2R_c \log_2 M)$. This is shown in Figure 4e and 4f.

Performance of Coded PPM

A full treatment of the subject of code design and performance is beyond the scope of this chapter. In lieu of the expanded discussion, we summarize the conventional approaches and recent advancements in the area and direct the reader to references where the complete details are contained.

Conventional Coded PPM Approaches

As mentioned earlier in this chapter, the initial PPM applications were analog in nature and, of course, did not use any coding. Shortly after quantized, now conventional, PPM became common in the literature, it was realized that an ECC could substantially improve performance.

Reed-Solomon (RS) *codes* (Lin and Costello 1983) were among the first codes proposed for use with PPM (McEliece 1981). An RS(n, k) code is a linear block code that encodes every block of k data symbols into n code symbols, where each symbol is an element of the Galois field with $q = n + 1$ elements, denoted GF(q) (Lin and Costello 1983). Most commonly, q is a power of 2, $q = 2^s$, in which case each symbol is conveniently represented by s bits. Thus, the code can also be viewed as a (sn, sk) binary code.

The beauty of RS-coded PPM is that the RS code symbols in GS(q) are a natural fit with the nonbinary nature of PPM signaling. One can use RS(n, k) with M-PPM, $M = n + 1$, by assigning each RS code symbol to one PPM symbol. On the other hand, if system constraints push one toward small M, this leads to small block-length codes that have limited coding gain. This problem can be overcome, in part, by using a longer RS code and splitting RS code symbols across multiple PPM symbols (Hamkins and Moision 2005).

Recent Advancements in Coded PPM: Serially Concatenated PPM

An ECC maps information bits to coded bits, whereas PPM maps these coded bits to PPM symbols. We may consider the combination of the code and modulation as a single large code that maps information bits directly to symbols transmitted on the channel. If the ECC is conducive to iterative decoding (Benedetto et al. 1996), then one effective technique for decoding the large code is to iteratively decode the modulation and the ECC.

Following this approach, codes have been developed for the deep space optical PPM channel that operate within 1 dB of the capacity limit (Moision, Hamkins, and Cheng 2006), several dB better than RS-coded PPM, and more than 1 dB better than turbo-coded PPM which does not iteratively demodulate the signal (Hamkins and Srinivasan 1998). A representative example of the *serially concatenated PPM* (SCPPM) code is shown in Figure 5. The code is the serial concatenation of a convolutional code, a bit interleaver, an accumulator (differential encoder), and PPM. The specific design involves optimizing the PPM order, code rate, and convolutional code, given the design constraints (Moision and Hamkins 2003). The code is decoded iteratively (Moision and Hamkins 2005, "Coded"), using standard turbo-decoding principles. The complexity may be reduced by discarding most of the slot likelihood ratios without noticeably affecting performance (Moision and Hamkins 2005, "Reduced"), and other complexity-reducing implementation techniques (Cheng, Moision, and Hamkins 2006) make it possible to produce a 50 Mbps decoder on standard FPGA hardware that became available in 2006.

The performance of various rate 1/2 codes on a Poisson channel is illustrated in Figure 6, along with channel capacity. The channel was set to $K_b = 0.2$ background photons per slot, which is typical for the existing MLCD-class design for reception from Mars. The SCPPM code performs within approximately 0.75 dB of soft decision capacity and well beyond the performance of hard decision capacity. There is a gap of 1.5 dB between hard decision and soft decision capacity for this channel. Recall from earlier that an approximate 2 dB gap exists between hard and soft decision decoding. The 2-dB gap is a rule of thumb that applies to a wide range of coded communications systems, but it is not a theorem. For the optical application, the gap between hard and soft decision decoding for the optical channel is not actually fixed; instead, it varies with the channel model and operating conditions. In fact, the hard and soft capacity gap for the Poisson channel is zero when $K_b = 0$, because hard and soft decisions are equivalent in that case; the gap increases to several dB with increasing K_b.

Figure 6 also shows the performance of two RS codes. The RS (63,31) code has symbols that are matched to the PPM order; it operates at approximately 4.25 dB from soft decision capacity when the BER is 10^{-6}. The longer block length RS (4095,2047) code reduces this gap to 3.7 dB. The gap remains several dB away from soft decision

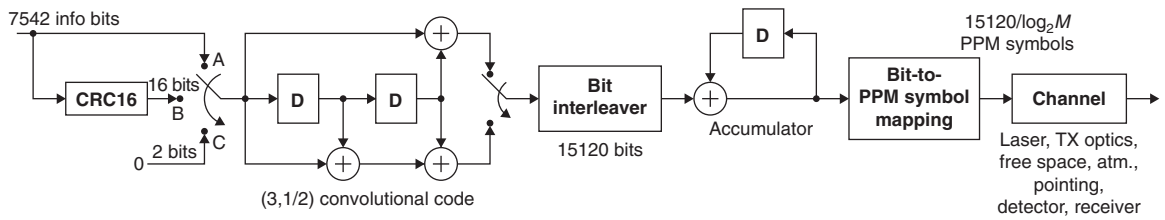

Figure 5: The SCPPM encoder

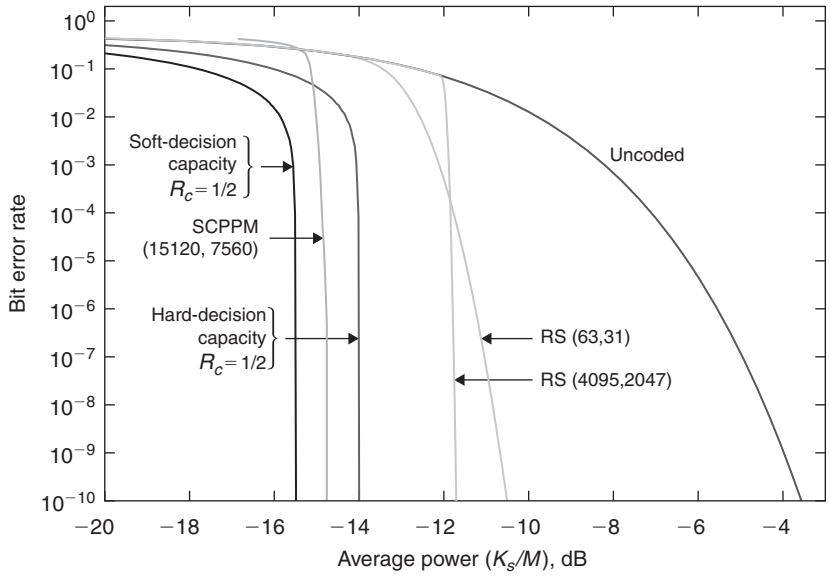

Figure 6: Performance of uncoded, RS-coded, and SCPPM-coded 64-PPM versus average power on a Poisson channel with $K_b = 0.2$

capacity, in part because of its use of hard decision decoding.

SYNCHRONIZATION

To detect symbols properly, a PPM receiver must acquire the PPM symbol timing—that is, identify the boundaries of the PPM symbols. The total timing may either be determined directly, or the problem may be partitioned into one of determining the slot timing and symbol timing sequentially. Figure 7 illustrates this for the case of 4-PPM. The transmitted PPM symbols in the upper part of the figure are misaligned by a slot offset and symbol offset at the receiver, shown in the lower part of the figure. The total timing error is the difference of the symbol offset and the slot offset.

Blind Synchronization

A *blind synchronizer* is one that operates without any knowledge of the PPM symbols being transmitted—that is, when no pilot or repetition signal is available. This is the case for any system in which transmitted PPM symbols consist solely of those that result from a modulation of coded or uncoded user data.

The PPM slot synchronization problem is closely related to the well-studied problem of symbol timing recovery of radio frequency *binary phase shift keying* (BPSK) signals. They both can be solved by arithmetically combining the energy detected in certain intervals of time in such a way that an error signal is generated that is proportional to the timing error. Two differences are that in PPM the signal energy is confined to a single slot among M slots instead of appearing in every slot, and the signal is on-off instead of antipodal.

For BPSK, timing recovery can be accomplished with a *digital transition tracking loop* (DTTL). For PPM, the analogue of the DTTL is a decision-directed slot recovery loop (Srinivasan, Vilnrotter, and Lee 2005), which is illustrated in Figure 8. As described in Srinivasan, Vilnrotter, and Lee (2005):

> A PPM signal delayed by the timing error $\Delta > 0$ is passed to the top branch that outputs the integrated slot values and selects the slot corresponding to the maximum value over an arbitrarily defined "pseudo-symbol." In the lower branch, the signal is further delayed by one symbol duration and passed to the error detector, which multiplies it by a "chopping function"—a square

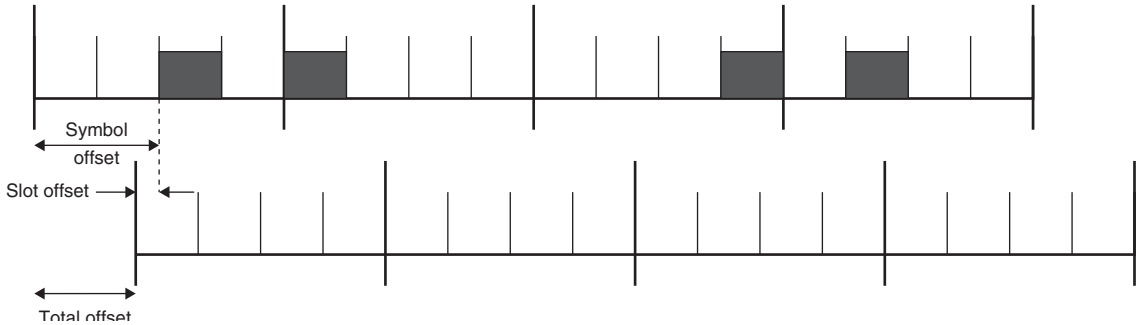

Figure 7: The transmitted symbols (top) result in a slot offset and symbol off set at the receiver (bottom)

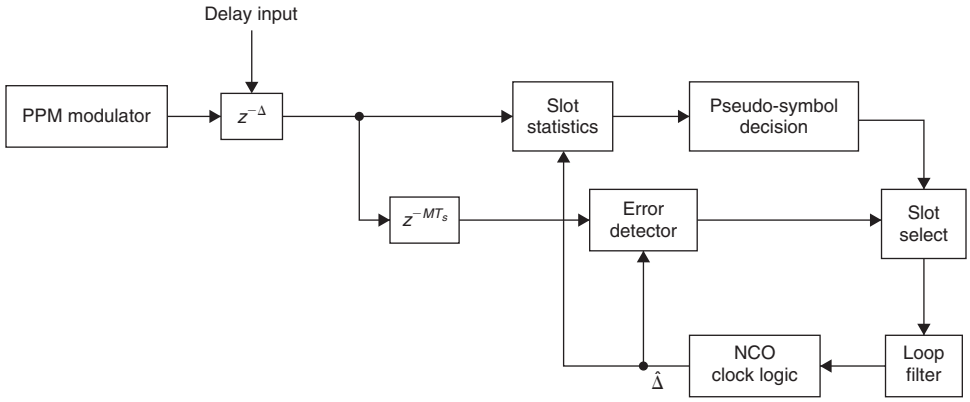

Figure 8: Decision-directed slot synchronization of PPM

> wave at the slot frequency—and integrates over the duration of a slot, each slot. The signal is then gated by the slot selector from the upper branch in order to create the timing error signal, which is filtered and then passed to the numerically controlled oscillator …, which outputs the slot clock. Note that symbol synchronization need not be assumed for this algorithm to work. If the initial pseudo-symbol interval contains two signal pulses, there will simply be two main contenders for the maximum slot to be picked by the slot selector, only one of which can be picked to contribute to the error detector. On the other hand, if the pseudo-symbol interval contains no signal pulse, a noise slot will be picked as the maximum, effectively increasing the symbol-error rate … in the PPM decision process.

Following slot synchronization, symbol synchronization is performed. If aligned, each PPM symbol will contain exactly one pulse. The number of signal pulses per (potentially misaligned) PPM symbol may be estimated by comparing slot values to a threshold. PPM symbol synchronization can be accomplished by, for example, comparing the slot offset that maximizes the number of PPM symbols having exactly one pulse exceeding the threshold.

In some designs, *dead time* is inserted between every PPM symbol. This can aid in symbol synchronization, because a correlation against the channel output will reveal no signal energy during the dead time. Dead time is sometimes needed in Q-switched laser communications, for example, to allow sufficient time for the laser to recharge before the next pulse is transmitted. Dead time does not cost the transmitter any power, but because it lowers the data rate it is usually avoided when possible.

Synchronization Using Pilot Tones

In some PPM applications (Lacy 1947), a *pilot tone* was transmitted along with the modulated pulses to simplify the synchronization process. A pilot tone is a series of reference pulses, perhaps even full PPM symbols, inserted throughout the PPM symbol stream. For example, a single known PPM symbol (e.g., $\mathbf{x}_1$) may be inserted after every nth PPM symbol. If there are s samples per slot, then M-PPM symbol synchronization is achieved by forming a length-sM vector sum of channel outputs over many blocks of sM samples. If the user data are random—that is, independent and equally likely a priori to take on any PPM value—then the samples in the slot corresponding to the pilot tone slot will have a disproportionately large correlation compared to the other slots. This accomplishes both slot and symbol synchronization in a low-complexity fashion.

Because a pilot tone is an unmodulated signal not representing any user in formation, its use reduces the efficiency of the transmission in terms of both bits per joule and bits per second. Therefore, the pilot tone is generally used as infrequently as the successful operation of the synchronization system allows. Also, care must be taken for uncoded PPM systems because the pilot signal might not be discernible in the presence of a string of all zeros in the user data—for example, as might occur in a raster scan of a dark area of an image.

CAPACITY OF PPM ON AN OPTICAL CHANNEL

Shannon (1948) demonstrated that for any communications channel, as long as the rate of transmitting information is less than some constant, C, it is possible to make the average error probability arbitrarily small by coding messages into a large enough class of signals. The constant C is called the *capacity* of the channel. Characterizing the capacity of the optical channel provides a useful bound on the data rates achievable with any coding scheme, serving as a benchmark for assessing the performance of a particular design.

The capacity will be a function of the received optical signal and noise powers, the modulation, and the detection method. The loss in capacity by restricting the modulation to PPM is small in the low average power regime where the deep space optical channel currently operates (Hamkins and Moision 2005; Wyner 1988; Boroson 2006).

We divide the capacity into two categories depending on the type of information provided to the decoder by the

receiver. In one case, the receiver passes hard PPM decisions on to the decoder. The hard decision capacity may be expressed as a function of the probability of uncoded PPM symbol error, P_s, derived for several channel models presented earlier. In the second case, the receiver passes soft log-likelihood ratios to the decoder. In this case, the soft decision capacity may be expressed as a function of the channel statistic $f_{Y|X}$. The soft decision capacity is at least as large as the hard decision capacity, as the slot counts provide additional information to the decoder.

General Capacity Formulas

The hard decision PPM channel is an M-ary input, M-ary output, symmetric channel with capacity given by (Gallager 1968):

$$C = \log_2 M + (1-P_s)\log_2(1-P_s) + P_s \log_2\left(\frac{P_s}{M-1}\right) \text{ bits per PPM symbol} \quad (21)$$

where P_s is the probability of incorrect PPM symbol detection, given by Equation 10 or Equation 13.

The soft decision capacity is given by (Moision and Hamkins 2003):

$$C = E_{\mathbf{Y}} \log_2 \left[\frac{ML(Y_1)}{\sum_{j=1}^{M} L(Y_j)}\right] \text{ bits per PPM symbol} \quad (22)$$

an expectation over $\mathbf{Y}$, where $L(y) = f_{Y|X}(y|1)/f_{Y|X}(y|0)$ is the channel likelihood ratio, the Y_j have density $f_{Y|X}(y|1)$ for $j = 1$ and density $f_{Y|X}(y|0)$ otherwise.

The M-fold integration in Equation 22 is often intractable. However, it is straightforward to approximate the expectation by a sample mean. A quick approximation follows from the lower bound

$$C \geq E \log_2 \left[\frac{M}{1+\frac{M-1}{L(Y_1)}}\right] \text{ bits per PPM symbol} \quad (23)$$

which is a good approximation for large M, reducing the M-fold integration (or set of M-dimensional vector samples) needed to evaluate Equation 22 to a one-dimensional integral (or set of scalar samples).

Capacity of PPM on Specific Channels

Poisson Channel

We consider first the Poisson channel. The behavior of the case $K_b = 0$ has a particularly simple form. When $K_b = 0$, we have

$$L(k) = \begin{cases} e^{-K_s} & k = 0 \\ \infty & k > 0 \end{cases}$$

and Equation 22 reduces to

$$C = (\log_2 M)(1 - e^{-K_s}) \text{ bits/PPM symbol}$$

When $K_b = 0$, only signal photons are detected. If any signal photons are detected, then the signal is known exactly. If no photons are detected, then all M candidate symbols are equally likely. Because the received statistic takes binary values, the soft and hard decision capacities are equal.

When $K_b > 0$, we have $e^{-K_s}\left(1+\frac{K_s}{K_b}\right)^k$, and Equation 22 becomes

$$C = (\log_2 M)\left(1 - \frac{1}{\log_2 M} E_{Y_1,\ldots,Y_M} \log_2 \left[\sum_{i=1}^{M}\left(1+\frac{K_s}{K_b}\right)^{(Y_j - Y_1)}\right]\right)$$

The case $K_b = 1$ is illustrated in Figure 9 as a function of average power (to within a constant factor) K_s/M for a range of M. In the plot, an average power constraint would be represented by a vertical line. A peak constraint can be shown (Moision and Hamkins 2003) to result in an upper limit on the PPM order. Hence, the maximum data rate subject to both peak and average power constraints can be identified using Figure 9.

AWGN Channel

For the AWGN channel, the likelihood ratio reduces to

$$L(y) = \sqrt{\frac{\gamma}{\beta+\gamma}} \exp\left[\frac{\beta \boldsymbol{\nu}^2 + 2\gamma\sqrt{\beta}\boldsymbol{\nu} - \gamma\beta}{2(\beta+\gamma)}\right]$$

where $\boldsymbol{\nu} = (y - m_0)/\sigma_0$ (recall that β and γ were defined earlier). The capacity reduces to

$$C = \log_2 M - E \log_2 \sum_{j=1}^{M} \exp\left[\frac{(V_j - V_1)\beta(V_j + V_1) + 2\gamma\sqrt{\beta}}{2(\beta+\gamma)}\right]$$

bits per PPM symbol, where $V_i = (V_j - m_0)/\sigma_0$ for $j = 1, \ldots, M$, or, when $\sigma_1 = \sigma_0$,

$$C = \log_2 M - E \log_2 \left[\sum_{j=1}^{M} e^{\sqrt{\beta}(V_j - V_1)}\right] \text{ bits per PPM symbol} \quad (24)$$

RELATED MODULATIONS

On-Off Keying

On-off keying (OOK) is another slotted modulation in which each slot contains either a pulse (1) or no pulse (0). In general, OOK allows any pattern of zeros and ones, and thus it is a generalization of several other modulation types. As such, the capacity of a channel using OOK is an upper bound on the capacity of a channel using one of its special case modulations. PPM is a special case of OOK, with the constraint that there is exactly one pulse

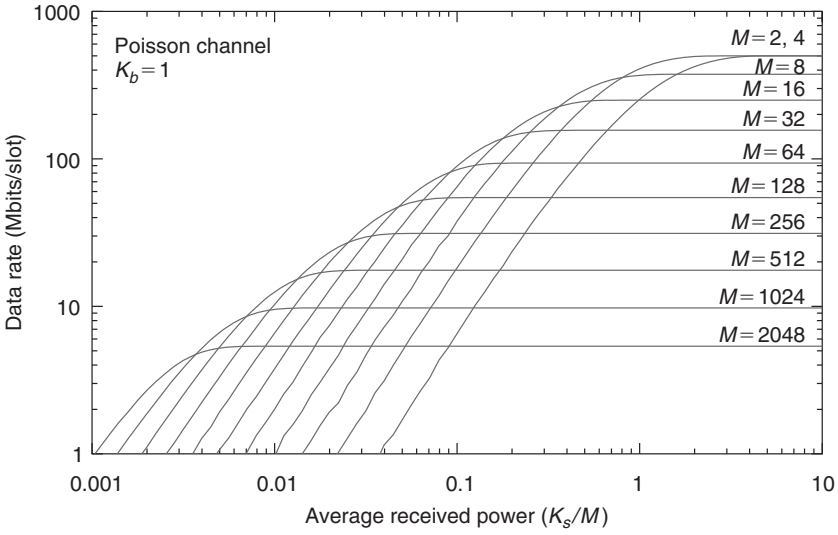

Figure 9: Capacity of M-PPM on a Poisson channel when $K_b = 1$

per M slots. Duty-cycle constrained OOK is another special case of OOK in which the fraction of slots with pulses is constrained to a specific number (Boroson 2006; Barron 2004). Duty-cycle constrained OOK is closely related to PPM, because each can have a duty cycle of $1/M$; it is also a generalization of PPM, because it does not require a frame of M slots to contain exactly one pulse.

Multipulse PPM

Multipulse PPM (MPPM), first proposed in Herro and Hu (1988), is a generalization of PPM that allows more than one pulse per symbol. In n-pulse M-slot MPPM there are n unique symbols that correspond to the possible ways to populate M slots with n pulses. This is illustrated in Figure 10 when $n = 2$ and $M = 8$. When $n > 1$, the mapping from message bits to MPPM symbols becomes more complicated, as $\binom{M}{n}$ is not a power of 2—that is, each multipulse symbol corresponds to a noninteger number of bits. This complication can be avoided by using a MPPM subset of size $2^{\left\lfloor \log_2 \binom{M}{n} \right\rfloor}$ (Sato, Ohtsuki, and Sasase 1994), which reduces throughput.

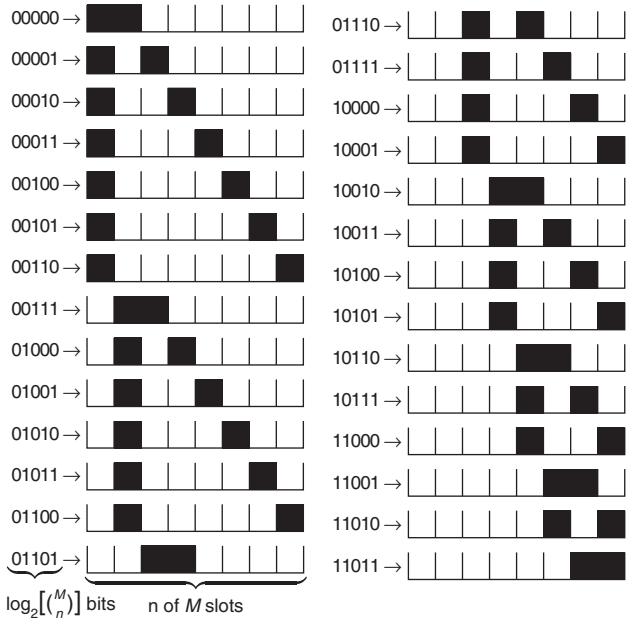

Figure 10: Two-pulse 8-ary PPM has $\binom{8}{2} = 28$ symbols

A recent result (Hamkins and Moision 2005) shows that in many cases of practical interest, the capacity of MPPM is not substantially greater than that of conventional PPM. The added complexity of implementing MPPM would not be justified in those cases. When the average power is sufficiently high, corresponding to an optimum PPM size of approximately 16 or less, then MPPM or more general modulations (e.g., Barron 2004) can begin to show power-saving gains of 1 dB or more over conventional PPM.

Overlapping PPM

Overlapping PPM (OPPM) is a generalization of PPM proposed in Lee and Schroeder (1977). In OPPM, each symbol interval of length T is divided into NM chips of duration $T_c = T/(NM)$. A pulse occupies N chips and is constrained to be entirely contained within the symbol epoch. This is shown in Figure 11 with $N = 3$ and $M = 4$. When $N = 1$, we have ordinary PPM as discussed above in which $\log_2 M$ bits are transmitted per T seconds. When $N > 1$, the pulse can be in one of $NM - N + 1$ positions (the last $N - 1$ positions are disallowed because the pulse must be completed contained within the symbol boundary), and we have $\log_2[NM - N + 1]$ bits per T seconds—that is, nearly an additional $\log_2 N$ bits per T seconds for large M. OPPM imposes more stringent synchronization requirements, and special synchronizable codes may be used to aid in this (Calderbank and Georghiades 1994).

Note that OPPM may result from a PPM modulation in which the slot width is accidentally or intentionally set too small. This can happen when the slot widths are defined too narrowly for the pulse width being transmitted or when the bandwidth of the detectors does not support the full resolution of the slot. Whatever the cause, the result is intersymbol interference. Even with perfect synchronization, the modulation set is not orthogonal, and

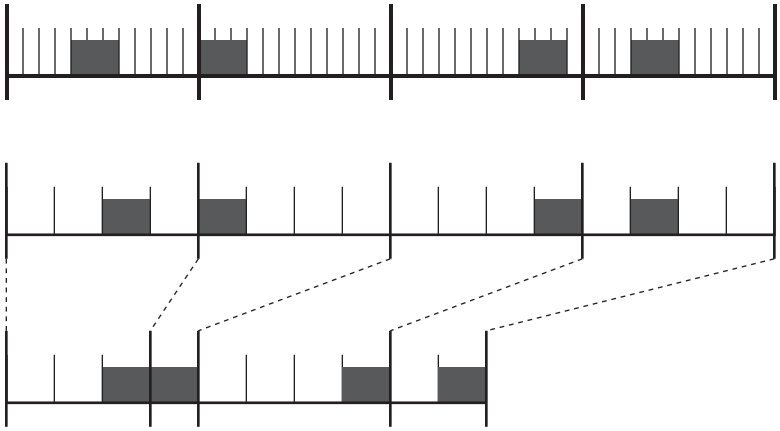

Figure 11: Each OPPM symbol with $N = 3$ and $M = 4$ has twelve chips. The pulse may begin in any of ten positions

Figure 12: A 4-ary PPM meassage (top) and the corresponding 4-ary DPPM message (bottom)

thus the raw SER performance will be degraded compared to PPM.

The intersymbol interference degradation may be mitigated with an ECC. This was recognized by Georghiades (1989), who proposed a trellis-coded modulation in conjunction with PPM and OPPM. The optimal receiver structure for this coded modulation involves a Viterbi decoder, and performance of this receiver for the AWGN and Webb channel models has been determined (Srinivasan 1998; Kiasaleh and Yan 1998).

Analog PPM

Analog PPM (Lacy 1947; McAulay 1968; Riter, Boatright, and Shay 1971; Ross 1949) may be viewed as the asymptotic limit of OPPM, in which the discrete chips that mark the permissible times at which a pulse may become infinitesimally narrow. In this way, the concepts of a slot and chip disappear entirely, and the pulse delay from the beginning of the symbol is simply an analog value. The position of a pulse is linearly related to the value of the analog message intended to be transmitted. For this modulation format, unless another synchronization method is provided, it may be necessary to transmit an auxiliary pulse to identify the beginning of each symbol.

The performance of such systems, in terms of the power efficiency or the effective information throughput achieved, is generally not comparable to conventional PPM with discrete slots, especially because an ECC is conceptually difficult to apply to an analog modulation format. However, this is compensated by the remarkable simplicity of the analog circuit that can measure the delay of the pulse. For the remote-controlled aircraft application mentioned early in the chapter, these lightweight receiver electronics are critical to a successful design, and analog PPM is often used. Several parameters—such as the position of the rudder, aileron, and elevators—can be independently controlled, and each parameter may take on infinitely many values.

Differential PPM

In *differential PPM* (DPPM) (Zwillinger 1988), also called *truncated PPM* (TPPM) and *digital pulse interval modulation* (DPIM), throughput is increased by beginning a new PPM symbol immediately following the slot containing the pulse. In other words, nonpulsed slots of a PPM symbol that follow a pulsed slot are flushed. This is shown in Figure 12. Information is conveyed in DPPM by the amount of separation between pulses. In one sense, this means that symbol synchronization is easier than in PPM: In PPM, the detection of a pulse does not assist much in determining the boundary of the PPM symbol, whereas in DPPM the symbol always sends with a pulse. On the other hand, the variable length of the symbols imposes a significantly more challenging synchronization problem than PPM because a missed pulse detection would lead to a *deletion* of a symbol from the symbol stream. Symbol deletions are generally fatal in both uncoded transmission (which is typically validated by a cyclic redundancy check) and to decoding algorithms. There may be methods of averting the synchronization problems with DPPM by buffering data and performing an appropriate sequence-detection algorithm. DPPM increases the throughput per unit time by almost a factor of two because symbols are on average only half as long as they would be with ordinary PPM.

Wavelength Shift Keying

From the viewpoint of communication theory, *wavelength shift keying* (WSK) (Dolinar et al. 2006), is similar to PPM of the same dimension. Instead of placing a single pulse of laser light of a given wavelength into one of M time-disjoint time slots, WSK places a single laser pulse of one of M disjoint wavelengths. This is shown in Figure 13. At the receiver, a filter bank completely separates the wavelengths before detection. Like PPM, this modulation is orthogonal. Therefore, if the channel is statistically

Figure 13: 4-ary WSK uses four frequencies in one time slot for each two bits

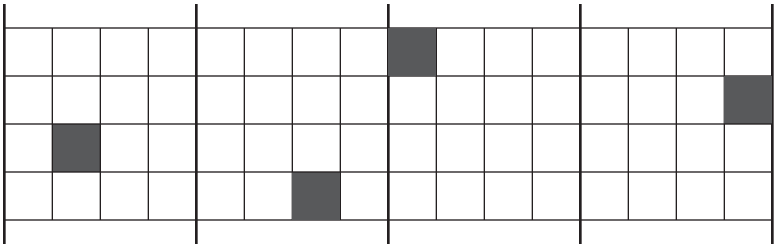

Figure 14: 4-ary WSK with 4-PPM uses four frequencies (in rows) and four times slots (in columns) for each four bits per symbol

identical at the various wavelengths, the maximum likelihood rules presented in the earlier section "Detection of PPM Signals" and the performance presented in the section "Performance of PPM" carry over to WSK as well.

Combined PPM and Wave Shift Keying

WSK transmits a pulse during every time slot. One way to reduce the required average laser power is to use a combination of PPM and WSK (Dolinar et al. 2006): By restricting the laser pulse to one of M time-slots, but allowing the laser pulse to take on any of N wavelengths, the low average laser power of conventional PPM can be maintained with the added advantage of increased data rate. This can be demonstrated by observing that the dimensionality of the signal space has been increased from M dimensions (PPM) to NM dimensions.

Combined PPM and WSK is an orthogonal signaling scheme. Therefore, if the channel is statistically identical at the various wavelengths, then the maximum likelihood rules presented in "Detection of PPM Signals" and the performance presented in "Performance of PPM" carry over to combined PPM and WSK as well (see Figure 14). The performance is the same as PPM, but with NM dimensions instead of M. The probability of correct detection is given by Equations 10 and 13, but with M replaced by NM.

The information throughput of this combined modulation scheme is $\log_2 NM = \log_2 N + \log_2 M$ bits per symbol period, or $\log_2 N$ more than M-PPM alone. For a given bandwidth, the throughput of combined PPM and WSK is higher than PPM alone. However, this modulation scheme requires N detectors, one for each wavelength, instead of just one. In addition, a method (e.g., high-dispersion grating) is needed to direct each distinct wavelength to a different detector.

CONCLUSION

Pulse position modulation is a modulation format with a rich set of applications in optical, radio frequency, and acoustical communications. The modern usage of PPM refers to a modulation format in which a binary input of $\log_2 M$ bits determines which of M slots is to have a pulse in it. This modulation has a high peak-to-average power ratio. The precise mapping of bits to PPM symbols may or may not affect performance, depending on the system; under typical circumstances, the maximum likelihood detection of a PPM symbol corresponds to the slot with the largest received value. A general formula for the capacity of PPM is known; thus, given bandwidth and power constraints, an appropriate near-capacity error-correcting code can be designed for many typical applications.

GLOSSARY

Channel capacity: The maximum mutual information between the input and output of a channel among all possible inputs to the channel. This determines the maximum data rate that is supportable by a given stochastic channel.

Gray code: An ordered set of binary vectors in which adjacent vectors differ in exactly one bit. An *anti-Gray code* is an ordered set of binary vectors in which adjacent vectors differ in either all positions or all but one position.

Maximum likelihood (ML) detection: The ML detection of a signal received from a channel is the value of the channel input that, among all possible channel inputs, maximizes the conditional probability density function of the observed channel output given the channel input.

Pulse position modulation (PPM): A signaling format in which the temporal positions of pulses are modulated by a message.

Reed-Solomon code: An error-correcting code popularly used with PPM signaling.

Serially concatenated PPM: An error-correcting code comprising the serial concatenation of a convolutional code, interleaver, and PPM.

Slot: An interval of time during which a 1 or a 0 is transmitted. In an optical communications application, a laser pulse would either be present or absent during this time interval.

Symbol error rate (SER): The probability that a symbol is detected in error, typically under the assumption of ML detection.

Symbol synchronization: The temporal alignment of a received stream of slots with the true symbol boundaries of the transmitted signal.

CROSS REFERENCES

See *Optical Fiber Communications*; *Wavelength Division Multiplexing (WDM)*.

REFERENCES

Agrell, E., J. Lassing, E. Strom, and T. Ottosson. 2004. On the optimality of the binary reflected Gray code. *IEEE Transactions on Information Theory*, 50(12): 3170–82.

Barron, R. J. 2004. Binary shaping for low-duty-cycle communications. *International Symposium on Information Theory* (ISIT), Chicago, June 22–July 2, p. 514.

Benedetto, S., D. Divsalar, G. Montorsi, and F. Pollara. 1996. A soft-input soft-output maximum a posteriori (MAP) module to decode parallel and serial concatenated codes. *TDA Progress Report*, 42(127): 1–20 (available at http://ipnpr.jpl.nasa.gov/progress_report/42-127/127H.pdf).

Biswas, A., and W. Farr. 2004. Detectors for ground-based reception of laser communications from Mars. In *Lasers and Electro-Optics Society* (*LEOS*), 1: 74–5.

Bornhoft, R., B. P. Brockway, M. Kunz, G. Lichtscheidl, B. Lindstedt, and P. A. Mills. 2001. Frame length modulation and pulse position modulation for telemetry of analog and digital data. U.S. Patent 6,947,795, issued October 2001.

Boroson, D. M. 2006. Private communication.

Calderbank, A. R., and C. N. Georghiades. 1994. Synchronizable codes for the optical OPPM channel. *IEEE Transactions on Information Theory*, 40: 1097–1107.

Candell, L. 2005. LDES: A prototype array optical receiver for the mars laser communications demonstration program. In *2005 Digest of the LEOS Summer Topical Meetings*, San Diego, July 25–27, 2005, pp. 13–14.

Casier, H., H. De Man, and C. Matthijs. 1976. A pulse position modulation transmission system for remote control of a TV set. *IEEE Journal of Solid-State Circuits*, 11(6): 801–9.

Cheng, M., B. Moision, and J. Hamkins. 2006. Implementation of a coded modulation for deep space optical communications. Information Theory and Applications Workshop, University of California at San Diego, February 6–10.

Dolinar, S., J. Hamkins, B. Moision, and V. Vilnrotter. 2006. Optical modulation and coding. Chap. 4 in *Deep space optical communications*, edited by H. Hemmati. New York: John Wiley & Sons.

Gagliardi, R., and S. Karp. 1976. *Optical communications*. New York: John Wiley & Sons.

———. 1995. *Optical communication*. New York: John Wiley & Sons.

Gallager, R. 1968. *Information theory and reliable communication*. New York: John Wiley & Sons.

Georghiades, C. N. 1989. Some implications of TCM for optical direct-detection channels. *IEEE Transactions on Communications*, 37: 481–7.

———. 1994. Modulation and coding for throughput-efficient optical systems. *IEEE Transactions on Information Theory,* 40: 1313–26.

Gray, F. 1953. Pulse code communication. U.S. Patent 2,632,058, issued March 1953.

Hamkins, J. 2004. Accurate computation of the performance of *M*-ary orthogonal signaling on a discrete memoryless channel. *IEEE Transactions on Communications*, 51(11): 1844–5.

———, M. Klimesh, R. McEliece, and B. Moision. 2004. Capacity of the generalized PPM channel. In *International Symposium on Information Theory* (ISIT), Chicago, June, p. 337.

———, and B. Moision. 2005. Multipulse pulse-position modulation on discrete memoryless channels, *IPN Progress Report,* pp. 42–161. http://ipnpr.jpl.nasa.gov/progress_report/42-161/161L.pdf.

———, and M. Srinivasan. 1998. Turbo codes for APD-detected PPM. In *Proceedings of the Thirty-Sixth Annual Allerton Conference on Communication, Control and Computing*, Urbana, Illinois, USA, September, pp. 29–38.

Herro, M. A., and L. Hu. 1988. A new look at coding for APD-based direct-detection optical channels. *IEEE Transactions on Information Theory*, 34: 858–66.

Kiasaleh, K., and T.-Y. Yan. 1998. T-PPM: A novel modulation scheme for optical communication systems impaired by pulse-width inaccuracies. *TMO Progress Report*, 42(135): 1–16 (available at http://ipnpr.jpl.nasa.gov/progress_report/42-135/135G.pdf).

Knutson, C. D., and J. M. Brown. 2004. *IrDA principles and protocols: The IrDA library*. Vol. 1. Salem, UT: MCL Press.

Lacy, R. E. 1947. Two mutichannel microwave relay equipments for the United States Army Communication Network. *Proceedings of the I.R.E. and Waves and Electrons*, 33: 65–9.

Lee, G. M., and G. W. Schroeder. 1977. Optical PPM with multiple positions per pulse width. *IEEE Transactions on Communications*, 25: 360–4.

Lee, S., G. G. Ortiz, and J. W. Alexander. 2005. Star tracker-based acquisition, tracking, and pointing technology for deep-space optical communications. *IPN Progress Report*, 42(161): 1–18. http://ipnpr.jpl.nasa.gov/progress_report/42-161/161L.pdf.

Lin, S., and D. J. Costello, Jr. 1983. *Error control coding: Fundamentals and applications*. Englewood Cliffs, NJ: Prentice Hall.

Marsh, L. M., C. Sun, B. K. Pillai, and L. Viana. 2002. Data recovery for pulse telemetry using pulse position modulation. U.S. Patent 6963290, issued November 2002.

McAulay, R. J. 1968. Numerical optimization techniques applied to PPM signal design. *IEEE Transactions on Information Theory*, 14: 708–16.

McEliece, R. J. 1981. Practical codes for photon communication. *IEEE Transactions on Information Theory*, 27: 393–8.

Meiseand, H. A., and V. R. DeStefano. 1966. A new self-contained private branch exchange utilizing electronic control and metallic crosspoints. *IEEE Transactions on Communications Technology*, 14: 763–7.

Moision, B., and J. Hamkins. 2003. Deep-space optical communications downlink budget: Modulation and coding. *IPN Progress Report*, 42(154): 1–28 (available at http://ipnpr.jpl.nasa.gov/progress_report/42-154/154K.pdf).

———. 2005. Coded modulation for the deep-space optical channel: Serially concatenated pulse-position modulation. *IPN Progress Report*, 42(161): 1–26 (available at http://ipnpr.jpl.nasa.gov/progress_report/42-161/161T.pdf).

———. 2005. Reduced complexity decoding of coded PPM using partial statistics. *IPN Progress Report*,

42(161): 1–20 (available at http://ipnpr.jpl.nasa.gov/progress_report/42-161/161O.pdf).

———, and M. Cheng. 2006. Design of a coded modulation for deep space optical communications. Information Theory and Applications Workshop, University of California at San Diego, February 6–10.

NEC Corporation. 1994. MOS integrated circuit μPD6121, 6122, NEC datasheet (retrieved from www.datasheetarchive.com/semiconductors/download.php?Datasheet=2205902).

Ohtsuki, T., and J. M. Kahn. 2000. BER performance of turbo-coded PPM CDMA systems on optical fiber. *Journal of Lightwave Technology*, 18: 1776–84.

Palais, J. C. 2004. *Fiber optic communication*s. 5th ed. Englewood Cliffs, NJ: Prentice Hall.

Pettit, R. 1965. Use of the null zone in voice communications. *IEEE Transactions on Communications*, 13(2): 175–82.

Press, W. H., S. A. Teukolsky, W. T. Vetterling, and B. P. Flannery. 1992. *Numerical recipes in C.* New York: Cambridge University Press.

Pulse position modulation technic. 1945. *Electronic Industries,* December, pp. 82–7, 180–90.

Riter, S., P. A. Boatright, and M. T. Shay. 1971. Pulse position modulation acoustic communications. *IEEE Transactions on Audio and Electroacoustics*, 19: 166–73.

Ross, A. E. 1949. Theoretical study of pulse-frequency modulation. *Proceedings of the I.R.E.*, 37: 1277–86.

Sato, K., T. Ohtsuki, and I. Sasase. 1994. Performance of coded multi-pulse PPM with imperfect slot synchronization in optical direct-detection channel. In *International Conference on Communications, Conference Record*, New Orleans, May 1–5, pp. 121–5.

Shannon, C. E. 1948. A mathematical theory of communication. *Bell Systems Technical Journal*, 27: 379–423, 623–56.

Srinivasan, M. 1998. Receiver structure and performance for trellis-coded pulse position modulation in optical communication systems. *TMO Progress Report*, 42(135): 1–11. http://ipnpr.jpl.nasa.gov/progress_report/42-135/135H.pdf

———, V. Vilnrotter, and C. Lee. 2005. Decision-directed slot synchronization for pulse-position-modulated optical signals. *IPN Progress Report*, 42(161): 1–12. http://ipnpr.jpl.nasa.gov/progress_report/42-161/161R.pdf

Tomkins, W. 2002. Smoke signals (retrieved from www.inquiry.net/outdoor/native/sign/smoke-signal.htm).

Townes, S., B. Edwards, A. Biswas, D. Bold, R. Bondurant, D. Boroson, J. Burnside, D. Caplan, A. DeCew, R. DePaula, R. Fitzgerald, F. Khatri, A. McIntosh, D. Murphy, B. Parvin, A. Pillsbury, W. Roberts, J. Scozzafava, J.Sharma, and M. Wright. 2004. The Mars laser communication demonstration. In *Proceedings of the IEEE Aerospace Conference*, 2: 1180–95.

Vilnrotter, V., M. Simon, and M. Srinivasan. 1999. Maximum likelihood detection of PPM signals governed by arbitrary point-process plus additive Gaussian noise. *IEEE Electronics Letters*, 34: 1132–3.

Webb, P. P., R. J. McIntyre, and J. Conradi. 1974. Properties of avalanche photodiodes. *RCA Review*, 35: 234–78.

Wilson, K., M. Jeganathan, J. R. Lesh, J. James, and G. Xu. 1997. Results from phase-1 and phase-2 GOLD experiments. *TDA Progress Report*, 42(128): 1–11 (available at http://ipnpr.jpl.nasa.gov/progress_report/42-128/128K.pdf).

Wilson, K. E., and J. R. Lesh. 1993. An overview of the Galileo Optical Experiment (GOPEX). *TDA Progress Report,* 42(114): 192–204 (available at http://ipnpr.jpl.nasa.gov/progress_report/42-114/114Q.pdf).

Wyner, A. D. 1988. Capacity and error exponent for the direct detection photon channel–Part II. *IEEE Transactions on Information Theory*, 34: 1462–71.

Zwillinger, D. 1988. Differential PPM has a higher throughput than PPM for the band-limited and average-power-limited optical channel. *IEEE Transactions on Information Theory*, 34: 1269–73.